THE STRUCTURE OF CORONAL PLASMA IN ACTIVE STELLAR CORONAE FROM DENSITY MEASUREMENTS

P. Testa[1,2], J. J. Drake[2] and G. Peres[1]

[1]Dip. Scienze Fisiche ed Astronomiche, Sezione di Astronomia, Università di Palermo, Piazza del Parlamento 1, 90134 Palermo, Italy

[2]Smithsonian Astrophysical Observatory, MS 3, 60 Garden Street, Cambridge, MA 02138

Abstract

We have analyzed high-resolution X-ray spectra of a sample of 22 active stars observed with the High Energy Transmission Grating Spectrometer (HETGS) on *Chandra* in order to investigate their coronal plasma density, using the lines of the He-like ions O VII, Mg XI, and Si XIII. Si XIII lines in all stars of the sample are compatible with the low-density limit (i.e. $n_e \leq 10^{13}$ cm^{-3}); Mg XI lines reveal the presence of high plasma densities up to a few 10^{12} cm^{-3} for most of the sources with higher X-ray luminosity ($\geq 10^{30}$ erg/s); O VII lines yield much lower densities of a few 10^{10} cm^{-3}. Our results indicate that the "hot" and "cool" plasma resides in physically different structures.

Our findings imply remarkably compact coronal structures, especially for the hotter (~ 7 MK) plasma emitting the Mg XI lines characterized by coronal surface filling factor, $f_{\rm MgXI}$, ranging from 10^{-4} to 10^{-1}, while we find $f_{\rm OVII}$ values from a few 10^{-3} up to ~ 1 for the cooler (~ 2 MK) plasma emitting the O VII lines.

Key words: Stars: activity, coronae, late-type – Sun: corona – X-rays: stars, spectroscopic plasma diagnostics

1. Introduction

X-ray and EUV spectra provide us with powerful tools for investigating the physics of the hot magnetically confined plasma in the outer atmospheres of late-type stars. The new generation X-ray observatories, *Chandra* and XMM-*Newton*, with their unprecedented spectral resolution and large effective areas, are providing us with high-resolution coronal X-ray spectra in which individual spectral lines can be readily resolved. The X-ray plasma diagnostics these spectra now allow for stars were previously accessible only for the Sun. The spectroscopic diagnosis of these astrophysical plasmas allows us to probe the physical conditions of the gas and to derive relevant parameters such as electron density, thermal structure, and relative element abundances, useful in order to eventually constrain models of the coronal heating and structuring.

The HETGS on *Chandra* (Canizares et al. 2000) provides high resolution ($\lambda/\Delta\lambda \sim 100 - 1000$) spectra in the energy range 1.5–30 Å (0.4–8.0 keV) where we observe a large number of prominent emission lines that provide useful plasma diagnostics (see also Testa et al. 2004a).

We analyzed the complexes of He-like "triplets" of O VII (22 Å), Mg XI (9.2 Å), and Si XIII (6.7 Å), which include the *resonance* line (r : 1s^2 ^{1}S$_0$ - 1s2p ^{1}P$_1$), the *intercombination* lines (i : 1s^2 ^{1}S$_0$ - 1s2p ^{3}P$_{2,1}$), and the *forbidden* line (f : 1s^2 ^{1}S$_0$ - 1s2s ^{3}S$_1$), corresponding to transitions between the $n = 2$ shell and the ground level, $n = 1$. The utility of these lines for plasma diagnostics was pointed out by Gabriel & Jordan (1969) (see also Porquet & Dubau 2000 for a recent treatment): the ratio $R = f/i$ is mainly density sensitive, owing to the metastable 1s2s ^{3}S$_1$ level, while the ratio $G = (f + i)/r$ is mostly temperature sensitive. Similar diagnostic techniques have been widely exploited for electron density estimates in EUV spectra (see, e.g., Mariska 1992 for solar applications, and, Laming 1998 for a review of stellar work). *Chandra* and XMM-*Newton* data offer the opportunity to apply these techniques to the X-ray range and to explore different temperature and density regimes. Analyses of He-like triplets seen in the X-ray spectra of a few different stars have appeared in the recent literature (e.g., Brinkman et al. 2000; Güdel et al. 2001; Huenemoerder et al. 2001; Ness et al. 2002; Stelzer et al. 2002). Several of these studies have outlined a general trend showing that plasma with temperatures of up to a few million K has densities similar to that found in solar active regions–up to a few 10^{10} cm^{-3} or so–while some evidence for higher density, even though controversial (see e.g. Brickhouse 2002), has been found from the analysis of hotter lines. For instance, the different resolving power of the available instruments might lead to a different effect of blending of other lines with the density-sensitive lines and differences in the determination of the continuum.

2. Observations and analysis

We have analyzed in detail the lines of Si XIII, Mg XI, and O VII observed with the *Chandra* HETGS, the best suited instrument for the analysis of these lines thanks to its high resolving power. Our sample (described in Tab. 1) comprises 22 late-type stars, covering a range of spectral types and activity levels in order to characterize the plasma physical conditions in stars with very different stellar parameters. We also probed possible trends of the plasma parameters with more global coronal parameters, such as

Table 1. List of stellar parameters.

Source	Spectral Type	$R_\star/R_\odot$	$M_\star/M_\odot$	$\log L_X$ [erg/s]
AU Mic	M1V	0.56	0.59	29.1
Prox Cen	M5Ve	0.16	0.11	26.7
EV Lac	M4.5V	0.41	0.34	28.5
AB Dor	K0V	1.	0.76	29.9
TW Hya	K8Ve	1.	0.7	30.1
HD 223460	G1III	13.6	2.9	31.8
31 Com	G0III	8	2.96	30.7
β Ceti	K0III	15.1	3.2	30.4
Canopus	F0II	53	13	30.5
μ Vel	G5III/..	13	3	30.2
Algol	B8V/K1IV	2.9/3.5	3.7/0.8	30.9
ER Vul	G0V/G5V	1.1/1.1	1.1/1.05	30.4
44 Boo	G1V/G2V	0.9/0.7	0.1/0.55	29.7
TZ CrB	G0V/G0V	1.1/1.1	1.12/1.14	30.5
UX Ari	G5V/K0IV	1.1/5.8	$\geq 0.6/\geq 0.7$	30.8
ξ UMa	G0V/G5V	0.95/..	0.9/..	29.1
II Peg	K2V/..	3.4/..	0.8/..	31.3
λ And	G8III/..	7.4/..	0.65/..	30.3
TY Pyx	G5IV/G5IV	1.6/1.7	1.22/1.20	30.7
AR Lac	G2IV/K0IV	1.8/3.1	$\geq 1.3/\geq 1.3$	30.8
HR 1099	G5IV/K1IV	1.3/3.9	1.1/1.4	31.0
IM Peg	K2III-II/..	13/..	1.5/..	31.4

X-ray luminosity or flux, or stellar effective temperature, gravity, rotational period, etc.

The Si, Mg and O He-like triplets are sensitive to temperature and density regimes in a wide range: 10 MK, 10^{13} cm^{-3} (Si XIII), 7 MK, 10^{12} cm^{-3} (Mg XI); 2 MK, 10^{10} cm^{-3} (O VII). We present here the analysis of plasma density while an analysis of the temperatures diagnostics (together with a more detailed discussion of the results presented here) can be found in Testa et al. (2004b).

Mg XI triplet region — The Mg XI triplet lines are likely to be affected by blending. Indeed, the APED database (Smith et al. 2001) predicts a number of Fe XIX–XXII lines in the 9.15–9.35 Å region, though each of these is considerably weaker than the Mg lines of interest. Moreover, lines from the Lyman series of H-like Ne with upper levels $n > 5$ also lie in this region. In order to take into account the possible blending with these lines we constructed an empirical model for the Mg XI region, considering additional components (Tab. 2). The model was constrained by comparison with, and by fitting to, co-added HEG spectra with the highest signal-to-noise ratio: β Ceti, TZ CrB, AR Lac and HR 1099. The fitting to this high S/N spectra (Fig. 1), allowed to constrain the relative position of the blending components. Line widths were all constrained to the same value, and the wavelength separations of the Mg XI triplet lines were fixed at their accurately known theoretical values.

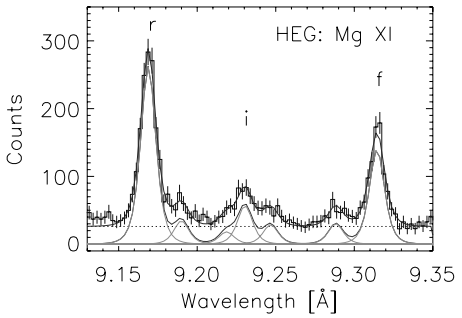

Figure 1. Coadded HEG spectra of four of the sources with the highest S/N: β Ceti, TZ CrB, AR Lac and HR 1099, with superimposed the best fit model with the blending components.

Table 2. Fitting Model: Mg XI lines and blending components.

λ_{obs} (Å)	Ion	transition	Emissivity (ph cm^{3}s^{-1})
9.1689	Mg XI	r: $1s2p\ ^1P_1 \rightarrow 1s^2\ ^1S_0$	1.10×10^{-16}
9.1900	Fe XXI	$1s^2 2s 2p_{1/2}^2 4p_{3/2} \rightarrow 1s^2 2s^2 2p^2\ ^3P_0$	1.14×10^{-17}
	Fe XX	$1s^2 2s 2p_{1/2} 2p_{3/2}^2 4p_{3/2} \rightarrow 2s^2 2p^3\ ^4S_{3/2}$	3.29×10^{-18}
	Ne X	10→1	1×10^{-18}
9.2187	Fe XX	$2s^2 2p^2(^3P)5d\ ^2F_{5/2} \rightarrow 2s^2 2p^3\ ^2D_{3/2}$	1.63×10^{-18}
	Ne X	9→1	1.4×10^{-18}
9.2304	Mg XI	i: $1s2p\ ^3P_{2,1} \rightarrow 1s^2\ ^1S_0$	1.60×10^{-17} 2.23×10^{-18}
9.2467	Ne X	8→1	2.1×10^{-18}
9.2882	Ne X	7→1	3.1×10^{-18}
	Fe XX	$2s^2 2p^2(^3P)5d\ ^4P_{5/2} \rightarrow 2s^2 2p^3\ ^2D_{3/2}$	2.82×10^{-18}
	Fe XXII	$1s^2 2s 2p(^3P)4d\ ^4D_{3/2} \rightarrow 1s^2 2s 2p^2\ ^2D_{3/2}$	1.37×10^{-18}
9.3144	Mg XI	f: $1s2s\ ^3S_1 \rightarrow 1s^2\ ^1S_0$	5.31×10^{-17}

2.1. Densities

We characterise the general R ratio and plasma density findings here as follows:

- R ratios and, consequently, plasma densities at temperatures of $\sim 10^6$ K are all very similar, with typical densities of $n_e \sim 2 \times 10^{10}$ cm^{-3} and a scatter between different stars of approximately a factor of 2 (Fig. 2).
- In all the stars studied, the observed Si XIII R ratios are above or similar to the predicted low density limit

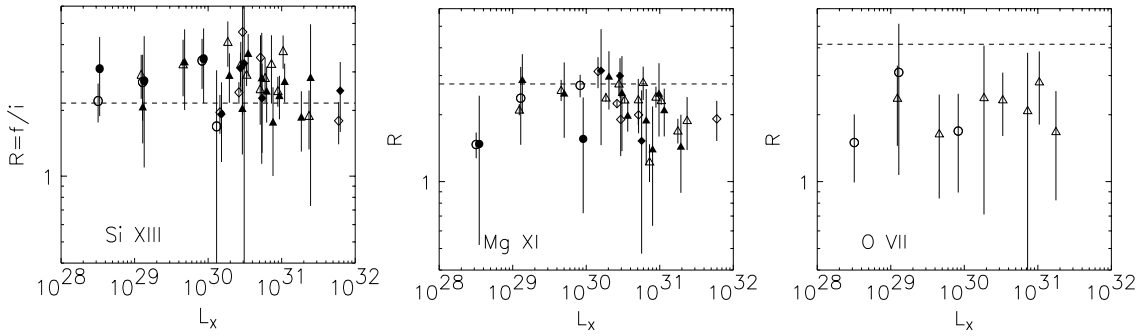

Figure 2. Measured R ratios for Si XIII*, Mg* XI*, and O* VII *vs. the X-ray luminosity. The dashed line marks the R value corresponding to the low-density limit; lower values correspond to higher density. Symbols as in Figure 3.*

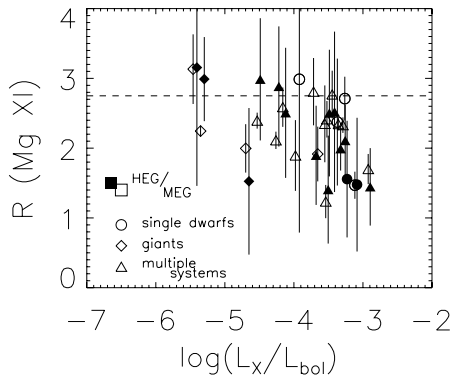

Figure 3. R ratios from the Mg XI *triplet vs.* L_X/L_{bol}.

(Fig. 2). At face value this indicates that no star has a coronal plasma density $\geq 10^{13}$ cm^{-3} at temperatures of $\sim 10^7$ K or higher. This result casts some doubt on earlier studies based on Fe XX- XXII lines seen in EUVE spectra which suggested the presence of densities exceeding 10^{13} cm^{-3} in active stellar coronae.

- Mg XI lines reveal the presence of high plasma densities up to a few 10^{12} cm^{-3} for several sources. We find a trend of higher plasma density in sources with higher coronal temperatures, and with higher coronal X-ray luminosities (Fig. 2). This trend is less obvious when cast in terms of surface flux, and more obvious when viewed as a function of the ratio of X-ray to bolometric luminosities (Fig. 3).

2.2. Filling factors

Insights into the structuring of the plasma and into the emitting volumes can be gained through density measurements. The density information can be used to investigate coronal filling factors:

$$f = \frac{V}{\mathcal{L}} \cdot \frac{1}{A_\star} = \frac{EM}{n_e^2 \mathcal{L}} \cdot \frac{1}{A_\star} = \frac{I_k^{\rm obs}}{n_e^2 G_k(T, n_e)} \cdot \frac{1}{\mathcal{L}} \cdot \frac{1}{A_\star},$$

provided an estimate of the characteristic scale height of the emitting plasma $\mathcal{L}$. We assume as characteristic scale height $\mathcal{L}$ the loop length derived from the scaling laws of an hydrostatic loop model such as that of Rosner et al. (1978) for which $L_{\rm RTV} \sim [T/(1.4 \times 10^3)]^3/p$.

Fig. 4 shows the filling factors derived from both Mg XI and O VII lines vs. the stellar X-ray surface flux. In order to have a more complete sample and investigate the relation with X-ray emission, we assumed n_e(O VII) = 2×10^{10} cm^{-3} for the stars whose O VII lines were not measurable (shaded symbols in plots).

- With some degree of scatter, the O VII filling factor, $f_{\rm OVII}$, is directly proportional to the X-ray surface flux, and it appears to saturate–i.e. reach values between 0.1 and 1–at a mean surface flux of $\sim 10^7$ erg cm^{-2} s^{-1}, the same found by Withbroe & Noyes (1977) for the areas of the solar surface covered with active regions. This suggests then, that at temperatures of up to a few 10^6 K these "O VII saturated" stars are essentially covered by active regions possibly similar in nature to those of the Sun.
- The behaviour of the Mg XI filling factor is different: there is a clear break in the $f_{\rm MgXI}$-F_X relation *at the same surface flux level,* $F_X \sim 10^7$ *erg s*$^{-1}$ *cm*$^{-2}$*, as we see* $f_{\rm OVII}$ *saturate.* At lower F_X levels, the $f_{\rm MgXI}$-F_X relation appears to have a shallower slope than that for $f_{\rm OVII}$ vs. F_X though the level of scatter precludes a definitive statement.

3. Discussion and conclusions

Atomic physics — Thanks to the unprecedented *Chandra* spectral resolution we have carried out an accurate analysis of the effect of lines blending with the Mg XI triplet

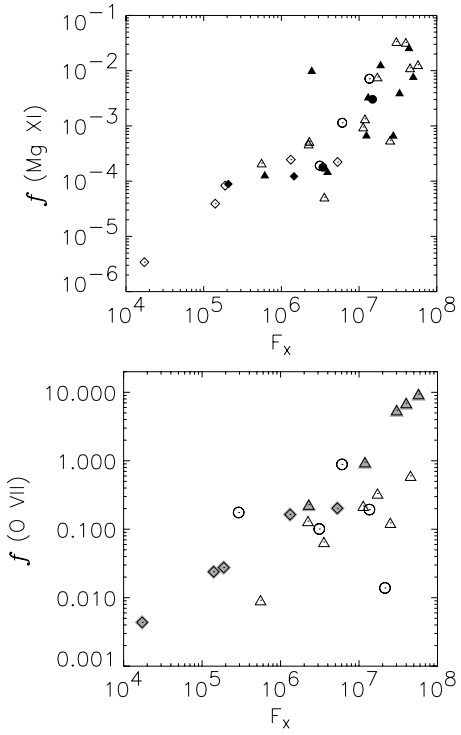

Figure 4. Surface filling factors derived from Mg XI *and O* VII *lines vs. X-ray surface flux. Symbols as in Figure 3.*

lines, in order to obtain reliable measurements of the R ratio. Our measured R ratios provide some insights into the propriety of recent theoretical calculations of the relative line strengths from He-like ions. In the case of Si XIII, we find some evidence suggesting that the low density limit f/i ratios predicted by both APED and Porquet et al. (2001) are too low by 20-40% or so based on our observed values (see Testa et al. 2004b for a detailed discussion).

Densities and correlations with stellar parameters — Our survey confirms the general finding of higher plasma densities at higher temperatures in active stars, already suggested by the analysis of several EUV and X-ray observations (e.g., Bowyer et al. 2000; Drake et al. 2001; Argiroffi et al. 2003). However, the upper limit of $n_{\rm e} \leq 10^{13}$ cm^{-3} imposed by Si XIII for *all stars of our sample* is not compatible with very high densities found from some Fe EUV line ratios (e.g. Sanz-Forcada et al. 2003a); inaccuracies in the theoretical Si XIII R ratio or influence of lines blending with the density-sensitive diagnostics might be responsible for the observed discrepancies.

We have found higher densities in more X-ray luminous coronae. A distinct correlation is also visible between the measured Mg XI R ratio and the X-ray "production efficiency", $L_{\rm X}/L_{\rm bol}$. No correlations were found between R ratio and stellar surface gravity, or effective temperature, or Rossby number.

Filling factors — The estimated surface coronal filling factors are significantly smaller for the hotter plasma ($T \sim 10^7$ K), with $f_{\rm MgXI} \sim 10^{-4} - 10^{-1}$, than for the cooler $\sim$ 2-3 $\times\, 10^6$ K plasma characterized by $f_{\rm OVII}$ values in the range $10^{-3} - 1$. The quite different gas densities found for "high" and "low" coronal temperatures reinforces the fact that the dominant emission at these temperatures cannot originate from the same structures: models seeking to explain active coronae need to account for the increase in gas pressure with increasing temperature.

Acknowledgements

PT was partially supported by *Chandra* grants GO1-20006X and GO1-2012X under the SAO Predoctoral Fellowship program. JJD was supported by NASA contract NAS8-39073 to the *Chandra X-ray Center*. GP and PT were partially supported by MIUR and by ASI.

References

Argiroffi, C., Maggio, A., & Peres, G. 2003, A&A, 404, 1033
Bowyer, S., Drake, J.J., & Vennes, S. 2000, ARA&A, 38, 231
Brickhouse, N.S. 2002, in ASP Conf. Ser. 277: Stellar Coronae in the *Chandra* and XMM-*Newton* Era, 13
Brinkman, A.C., Gunsing, C.J.T., Kaastra, J.S., et al. 2000, ApJL, 530, L111
Canizares, C.R., Huenemoerder, D.P., Davis, D.S., et al. 2000, ApJL, 539, L41
Drake, J.J., Brickhouse, N.S., Kashyap, V. et al. 2001, ApJL, 548, L81
Güdel, M., Audard, M., Briggs, K., et al. 2001, A&A, 365, L336
Gabriel, A.H. & Jordan, C. 1969, MNRAS, 145, 241
Huenemoerder, D.P., Canizares, C.R., Schulz, N.S. 2001, ApJ, 559, 1135
Laming, J.M. 1998, in ASP Conf. Ser. 154: Cool Stars, Stellar Systems, and the Sun, 447
Mariska, J.T. 1992, The solar transition region (Cambridge Astrophysics Series, NY: Cambridge University Press, 1992)
Ness, J.-U., Schmitt, J.H.M.M., Burwitz, V., et al. 2002, A&A, 394, 911
Porquet, D., Mewe, R., Dubau, J., Raassen, A.J.J., & Kaastra, J.S. 2001, A&A, 376, 1113
Porquet, D. & Dubau, J. 2000, A&AS, 143, 495
Rosner, R., Tucker, W.H. & Vaiana, G.S. 1978, ApJ, 220, 643
Sanz-Forcada, J., Brickhouse, N.S., & Dupree, A.K. 2003, ApJS, 145, 147
Smith, R.K., Brickhouse, N.S., Liedahl, D.A. & Raymond, J.C. 2001, ApJL, 556, L91
Stelzer, B., Burwitz, V., Audard, M., et al. 2002, A&A, 392, 585
Testa, P., Drake, J.J., Peres, G. & E.E. DeLuca 2004, ApJL, 609, L79
Testa, P., Drake, J.J. & Peres, G. 2004, ApJ, in press
Withbroe, G.L. & Noyes, R.W. 1977, ARA&A, 15, 363